RSC Advances

ROYAL SOCIETY OF CHEMISTRY

www.rsc.org/advances

Journal Name

ARTICLE

Fabrication of AgBr Nanomaterials As Excellent Antibacterial Agent

Received 00th January 20xx,
Accepted 00th January 20xx

DOI: 10.1039/x0xx00000x

www.rsc.org/

Zhouzhou Liu,[#a,b] Wei Guo, [#a,b] Chongshen Guo[a]* and Shaoqin Liu[a]*

Nanoparticle of sparingly soluble silver salt of AgBr with an appropriate solubility product and high photocatalytic response ought to be a promising candidate with superior and multifunctional antibacterial effects, but it still undergoes relative less scientific attentions until now. In the present study, antibacterial activities of AgBr nanocube and its derivative Ag@AgBr against *E. coli* were investigated both in the dark and under visible light irradiation. Benefiting from a "dual punch" of eluted Ag^+ induced disturbances on bio-functions and nanocubes induced contact damage on cellular membrane, the 100 nm well-defined AgBr nanocubes realized the outstanding antibacterial properties, with MIC and MBC values being as low as 0.1 μg/ml and 0.4 μg/ml, respectively. Ag decoration on the surface of AgBr seems to deteriorate the antibacterial properties as the MIC and MBC values increased to 0.75 μg/ml and 1 μg/ml in the dark for the sample of Ag@AgBr, but it do exhibit the better photocatalytic inhibition on *E. coli* growth than pure AgBr in virtue of the enhanced light-harvesting by LSPR effect from Ag component. Thus, these encouraging results showed in this study manifest great potential of AgBr nanomaterial severing as an antibacterial candidate with high antibacterial activity.

1. Introduction

Wide-spread dispersion of various pathogenic microorganisms (such as bacteria, virus and fungi) in the water sources, food, sanitation and so forth, is one of the most mortal threats to the healthy setting of human.[1] As many bacterial strains today are resistant to antibiotics,[2-4] it strongly calls for powerful antibacterial agents with broad-spectrum antimicrobial properties for disinfection.[5]

In general, antibacterial agents discovered to date could be classified into three catalogues, that are natural, organic and inorganic agents.[6] Natural antibacterial agents refer to the compounds being often extracted from plants, animals and marine organisms, which are difficult to be highly scalable applications.[7] As to organic antibacterial agent, it usually suffers from poor thermal stability, low chemical stability, short durability, high toxicity.[8] As compared with organic and natural agents mentioned above, inorganic antibacterial agents exhibiting better performance in durability, heat resistant, and low occurrence of antibiotic-resistant bacterial strains, are attracting increasing attentions in recent years.[9-10] Among various inorganic antibacterial agents already discovered, silver-based materials are of special interests owing to their broad-spectrum inhibitory and bactericidal effects.[11-13] Employment of silver-based materials for the application of anti-microbial is roughly divided into the Ag nanoparticles and Ag salt. [14-19] In regard to Ag nanoparticles, Ag^+ is released from nanoparticles by a slow two-step oxidation process, as explained by the following equations:

$$4\ Ag + O_2 = 2\ Ag_2O \qquad \text{Eqn. 1}$$

$$2\ Ag_2O + 4H+ = 4\ Ag+ + 2\ H_2O \qquad \text{Eqn. 2}$$

and the dissolution kinetics relies on the size of the nanoparticles, surface functionalization, oxygen content, temperature, pH value and the composition of the surrounding medium.[20-21] Hence, according to the equation 1 and 2, if dissolved oxygen is completely removed, there is almost no dissolution of Ag^+ from silver nanoparticles. Therefore, application of silver nanoparticles as bactericidal agent is a slow process accounting for long-term effectivity, but it suffers low concentration of effective silver ions. In contrast, high solubility of silver salt, in most cast refers to silver nitrate,[22] can give rise to a high local available Ag^+ concentration, which kills bacteria at the cost of damage on the surrounding normal tissue as well. [1] To overcome this shortcoming, soluble silver salts are often loaded on the substrate, such as zeolites,[23-24] TiO_2,[25] silica[26] and carbon fiber,[27] for controlling the release rate of biocidal Ag ions from Ag-loaded materials. As a result, it is extremely important to seek for new antibacterial candidates, which can combine the advantages of high available silver concentration as silver salt and long-term effectivity as silver nanoparticles.

Fortunately for us, nanoparticle of sparingly soluble silver salts such as AgX (X= Cl, Br, I) with an appropriate solubility product

[a] Key Laboratory of Microsystems and Micronanostructures Manufacturing (Ministry of Education), Harbin Institute of Technology, Harbin 150080, P. R. China.
[b] School of Life Science and Technology, Harbin Institute of Technology, Harbin, 150080, P. R. China.
[c] E-mail: shaoqinliu@hit.edu.cn; chongshenguo@hit.edu.cn; Tel;+86 451 86403493
† # Equal contribution from Zhouzhou Liu and Wei Guo
Electronic Supplementary Information (ESI) available: [EDS results and TEM image of SiO_2]. See DOI: 10.1039/x0xx00000x

can act as Ag^+ reservoir to be persistent releasing sufficient Ag^+ in various conditions, resulting in high local Ag^+ concentration for killing the bacteria. What is more, nanoparticles of AgX readily present in stable colloidally form by controlling the size, morphology, and modification on surface conditions, therefore, it is expected to be able to penetrate the cell membrane and induce antibacterial effect.[1] Among these silver halides, AgBr nanoparticle has attracted much more attentions than other kind of sparingly soluble silver salts owing to its unique optical properties.[28-29] Response to visible light and spontaneous conversion to plasmonic Ag nanoparticle after exposure to even visible light motivated scientists to pay more attention on its photocatalytic properties, such as photocatalytic degradation of organic pollutants.[30-34] However, the efforts worked on investigating either the intrinsic antibacterial activities of pure AgBr in the dark or photo-destruction of microorganisms via photocatalytic process were relatively less. In this work, antibacterial activities of AgBr and its derivative of Ag@AgBr against *E. coli* were investigated both in the dark and under visible-light irradiation. AgBr nanoparticles have firstly been synthesized by a facile solution-based method involving employing PVP as capping agent. Afterwards, it could be converted to Ag@AgBr core-shell structure via reduction reaction by $NaBH_4$ in aqueous solution. Finally, the antibacterial properties and antibacterial mechanism of obtained samples were systemically investigated in this work.

2. Experimental

2.1 Synthesis of the AgBr nanocubes

Firstly, 5 mL of 0.1 M NaBr solution was added into 50 mL of 10 mM PVP solution to form a clear mixed solution, and then 5 mL $AgNO_3$ solution (0.1 M) was injected dropwise by peristaltic pump at a speed of 1 mL/min under intensive magnetic stirring. After that, the obtained solution was transferred to a Teflon-lined autoclave and kept at 120 ^oC for 12 hours. Finally, the AgBr nanoparticles were centrifuged and washed with deionized water and ethanol to remove residual unreacted reagents. What is notable, the washing and vacuum drying procedures were conducted in the dark during the overall process for avoiding formation of Ag or Ag_2O in our AgBr sample.

2.2 Synthesis of the Ag@AgBr nanoparticles

10.48 mg $NaBH_4$ was dissolved in 25 mL icy deionized water. Then, the resulting $NaBH_4$ solution was added into 100 ml AgBr nanocubes dispersion solution (1mg/ml) dropwise under intensive magnetic stirring. The color of the mixed solution turned from milky white to black at the end of dropping process. Finally, Ag@AgBr nanoparticles were obtained by centrifugation, washing with deionized water and ethanol, drying at room temperature overnight.

2.3 Antibacterial test

Escherichia Coli 8099 was activated in nutrient broth and diluted to ~10^5 cfu/mL by 0.03 M PBS buffer containing 0.1 % tween-80. Growth kinetics curves of *E. coli* cells against the antibacterial reagent of AgBr or Ag@AgBr were conducted in nutrient broth. 95 mL nutrient broth and 5 mL *E. coli* suspension were added into conical flask, and then added proper volume of AgBr dispersion to make the final concentration in the range of 0-1000 ppb. Then, the conical flask was incubated in gas bath thermostatic vibrator at 37 ^oC and 150 rpm. To test the optical density at different foster time, 200 uL of the broth was added into the 96-well plate, and the optical density of solution was obtained by microplate reader at 600 nm. Bacterial growth rates were determined according to the optical density at 600 nm (OD_{600}). The growth curve was obtained by plotting the optical density versus the foster time. For each concentration of AgBr or Ag@AgBr sample, trials were conducted 3 times in parallel. In this work, the minimal inhibition concentration (MIC) was defined as the lowest concentration of AgBr nanoparticle for completely inhibiting the bacterial growth within 12 h. Meanwhile, the minimum bactericidal concentration (MBC) refers to the lowest concentration of AgBr nanoparticles leading to no growth of *E. Coli* within the test period.

2.4 Dehydrogenase activity test

This work also examined the antibacterial mechanism by a TTC-color test according to Chen's work.[35] To put it simply, triphenyltetrazolium chloride (TTC) is a small and colorless matter that can be ingested by live bacteria and converted to red triphenylformazane (TF) when TTC catches the hydrogen atom produced by dehydrogenase of living *E. coli*. Hence, the intensity of red color is direct proportion to the number of liver bacterial. By this way, the variation trend on viability and dehydrogenase activity of *E. coli* after contact with AgBr nanoparticles could be qualitative described by optical absorption at 492 nm.

A cell suspension of 10 mL with a concentration of 10^6 cfu / mL and a proper volume of AgBr (final concentration 10 ppb) were mixed beforehand. After different contact time, the *E.coli* cells were separated from AgBr nanocubes by centrifugation at 3000 rpm for 5 min, and diluted into 5 mL suspension. The above separated *E.coli*, 5 mL Tris-HCl buffer (pH = 8.4) and 1 mL 1mg/mL TTC solution were added into a PE tube and incubated at 37 ^oC for 30 min. Afterwards, 2 mL H_2SO_4 was introduced into the solution to cease the enzyme reaction, and then added 5 mL $CHCl_3$ to extract TF for 10 min. The $CHCl_3$ extraction liquid was obtained by centrifugation at 3000 rpm for 5 min. Finally, the extraction liquid was colorimetric at 492 nm. The concentration of AgBr was 10 ppb, and the contact time between *E.coli* and AgBr was set to 0, 30, 60, 90, 120, 150 and 180 min, respectively. For each contact time, the trials were conducted 3 times in parallel. At the same time, the absorption at 492 nm of a control system without AgBr was also measured.

2.5 Galactosidase activity test

This test is based on the fact that leaking of β-D-galactosidase from bacterial cells, as a results of cell membrane damage inducing by antibacterial agent, will catalyze the hydrolysis o-nitrophenol,β-D-galactopyranoside to form o-nitrophenol, which has a characteristic absorption peak at 420 nm. Consequently, optical absorptivity at 420 nm can reflect the

antibacterial activities of nanoparticles and integrality of cell membrane.

A cell suspension of 5 mL with a concentration of 10^6 cfu/mL and 5 mL of ONPG solution with a concentration of 25 mmol/L were added simultaneously into 40 mL PBS buffer solutions (pH = 6.5). After shaking for 5 min, a proper volume of AgBr (final concentration was 10 ppb) was added into the cell suspensions containing ONPG and *E.coli*. The changes of optical density at 420 nm (OD420) with time were measured. At the same time, the OD_{420} of a control system without AgBr was also measured.

2.6 LIVE/DEAD fluorescence image

The antibacterial activity of AgBr nanoparticles was further verified by LIVE/DEAD BacLight bacterial viability assay (Invitrogen, USA). SYTO 9 and propidium iodide (PI) were used to stain the living and dead *E. coli* cells, respectively. The mixtures were incubated at room temperature in the dark for 15 min and then observed by OLYMPUS DP72 fluorescence microscope.

2.7 SEM Characterization on E.coli

In brief, *E. coli* without or with AgBr nanoparticles treatment were collected by centrifugation firstly. The obtained *E. coli cells* were fixed in 2.5% glutaraldehyde for approximately 20 min at ambient temperature, and then the samples were dehydrated by successive soakings in 37%, 95% and 100% ethanol each for 10 min, respectively. Finally, the resultant samples were dried naturally at room temperature. The morphologies of the *E. coli* cells were observed by scanning electron microscope.

2.8 MTT assay

The assay was performed out in triplicate in the following manner. For MTT assay, L02 human hepatocytes were seeded into 96-well plates at a density of 1×10^4 per well in 200 µL of media and grown overnight. The cells were then incubated with various concentrations of AgBr or Ag@AgBr for 24 h. Following this incubation, cells were then incubated in media containing 20 µL 5 mg mL^{-1} of MTT for another 4 h. After that, the media with MTT was removed, and 150 µL of DMSO was added to dissolve formazan crystal at room temperature for 30 min and the absorbance was measured at 490 nm by multi-detection microplate reader (SynergyTM HT, BioTek Instruments Inc, USA).

2.9 Characterizations

Field-emission scanning electron microscopy (FE-SEM) images were obtained using a Helios Nanolab 600i. The crystal phase of nanoparticles was determined by X-ray diffraction analysis (XRD, Panalytical Empyrean). The elemental analysis and chemical valence of sample were measured by X-ray photoelectron spectroscopy (XPS, ESCALAB 250Xi, Thermo Fisher Scientific), and the XPS peaks have been calibrated according to the C1s line. The optical response of solutions was performed on HITACHI U-4100 Spectrophotometer.

3. Results and discussion

3.1 Investigation on antibacterial activity of AgBr nanocubes

In this work, synthesis of AgBr nanoparticles was carried out by precipitation of $AgNO_3$ and NaBr in a PVP solution at ambient temperature and then followed by a hydrothermal treatment at 120 °C for further crystallization. Although several works reported the synthesis of AgBr nanoparticles just via one step of precipitation reaction,[31,32,34] the reason why an additional hydrothermal treatment was performed in this work is due to that the AgBr nanoparticles tended to be aggregation and became un-dispersable after drying if free of hydrothermal treatment. Fig. 1a shows the typical low-magnification SEM image of as-prepared AgBr nanoparticles of this work, from which we can clearly see that the AgBr sample consists of many monodispersed nanoparticles with well-defined cubic shape. The high-magnification SEM image, as shown in Fig. 1b, reveals that the size of these nanocubes is around 100 nm and the surface of nanocubes is covered by many tiny particles. The formation process of tiny particles on the surface of nanocube happened during SEM observation when the electron beam focused on the sample area. It is easily to understand that these tiny particles are metallic Ag particles as AgBr is well-known photosensitive substance and even could be reduced by daylight to form metallic Ag, let alone high-power electron beam under SEM conditions. This phenomenon warned us to do all of operations in the dark for avoiding formation of Ag@AgBr in this step. The crystal phase of AgBr nanoparticle was determined by X-ray diffraction analysis and the result is presented in Fig. 3c. The diffractive peaks locating at 2Θ = 26.725°, 30.96°, 44.346°, 55.04°, 64.476°, 73.261° could be well indexed to the AgBr crystal planes of (1 1 1), (2 0 0), (2 2 0), (2 2 2), (4 0 0), (4 2 0), respectively, and no impurity peaks have been found. The typical X-ray photoelectron spectrum for the core level of silver 3d is shown in Fig. 1d. The XPS curve is typical of one spin-orbit doublet for Ag^+ 3d 5/2 at 367.77 eV and Ag^+ 3d 3/2 at 373.8 eV, suggesting the element Ag in the sample is mainly in the form of AgBr and metallic Ag is absent or negligible. Combing with XRD results, it can be concluded that the nanocube of this work is

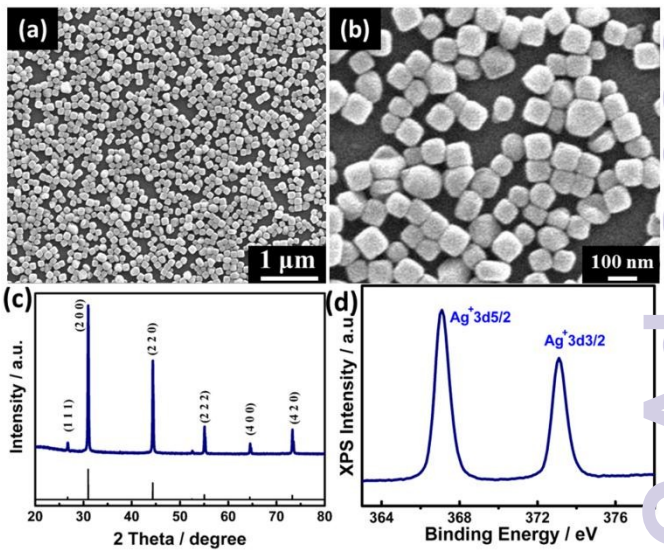

Figure 1 (a) Low magnification SEM image, (b) high magnification SEM image, (c) XRD diffraction pattern and (d) XPS spectra of as-prepared sample under hydrothermal condition at 120 °C for 12 h.

pure phase of AgBr and free of the Ag coating, which is highly necessary for investigating the intrinsic antibacterial properties of pure AgBr next.

Fig. 2 presents the growth kinetics curves of *E. coli* cells exposed to different concentrations of AgBr nanocubes. In general, the antibacterial activities on *E. coli* bacteria are direct proportion to the concentration of AgBr nanocubes provided in the incubating condition. Reduction on growth maximum of *E. coli* can be observed even at a concentration as low as 0.05 μg/ml, but there is no influence on delaying abrupt point of growth curve. When *E. coli* cells exposed to more AgBr nanocube as 0.1, 0.25, 0.3 μg/ml, abrupt points on the growth curves were lagged to 12, 16, and 20 h, respectively. Further increased the concentration of AgBr nanocube over 0.4 μg/ml, no growth of *E. coli* was confirmed. In this work, the minimal inhibition concentration (MIC) is defined as the lowest concentration of AgBr nanoparticles for completely inhibiting the bacterial growth within 12 h. Meanwhile, the minimum bactericidal concentration (MBC) refers to the lowest concentration of AgBr nanoparticles leading to no growth of *E. Coli*. In this way, the MIC and MBC values of AgBr nanocubes against *E. coli* are 0.1 μg/ml and 0.4 μg/ml, respectively. To strictly certify that the 0.4 μg/ml is the MBC values of AgBr nanocubes, *E. coli* cells before and after exposed to 0.4 μg/ml AgBr for 24 h underwent LIVE/DEAD BacLight bacterial viability assay in which living *E. coli* cells were stained with SYTO 9 to give a green color and dead *E. coli* cells were stained with propidium iodide to give a red color. As is shown in Fig.3, in the control tests of the *E. coli* cells without contact with AgBr nanocube or *E. coli* cells in contact with non-bactericidal nanoparticles of SiO_2, bright green stained patterns were observed, indicating *E. coli* cells are survival. In a sharp contrast, the *E. coli* cells were dead with red color after incubation with 0.4 μg/ml AgBr for 24 h. Statistical counting results based on fluorescence microscopic images verified that the AgBr nanocubes of 0.4 μg/ml killed more than 99% of *E.coli* with 24 h contact. By comparison with previous work, MIC and MBC values of AgBr nanocube against *E. coli.* are confirmed to be much lower than the reported Ag nanoparticles with MIC value of 6.25-33.71 μg/ml and MBC values of 12.5-20 μg/ml, Ag^+ with MIC value of around 3.5 μg/ml and MBC values of 3.5-5 μg/ml, Ag_2S nanoparticles with MIC value of >150 μg/ml, AgCl with MIC value of

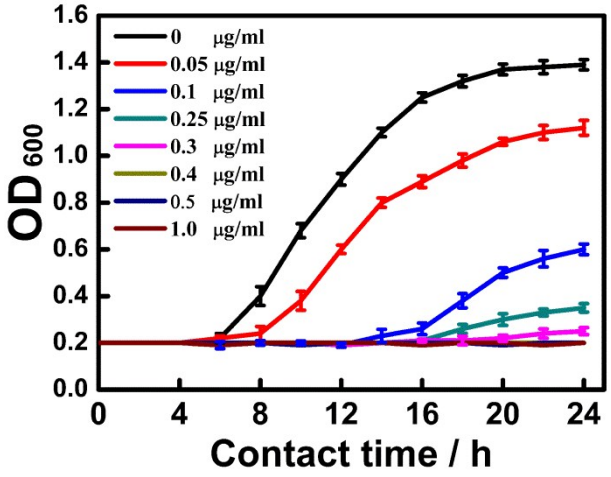

Figure 2 Growth curves of *E. coli* cells exposed to different concentrations of AgBr nanocubes (The *E. coli* bacterial grew in the nutrient broth).

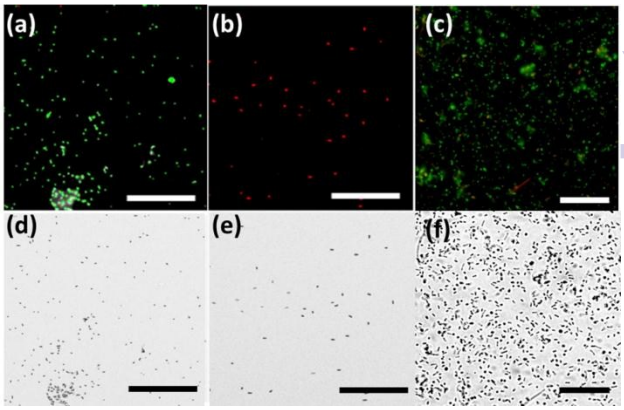

Figure 3 Fluorescence microscopic images of (a) *E. coli* cells, (b) *E. coli* cells exposed to 0.4 μg/ ml AgBr for 24 h, (c) *E. coli* cells exposed to 0.4 μg/ ml 50 nm SiO_2 for 24 h; (d) - (f) are real microscopic images corresponding to the (a)-(c), respectively. (The viability of *E. coli* was characterized by using the live/dead assay, where the living *E. coli* c were stained with SYTO 9 to give a green color and dead *E. coli* cells were stained with propidium iodide to give a red color). Bar inside the each image is 50 μm.

>0.5 μg/ml, manifesting the excellent and promising antibacterial properties of AgBr nanocube.[5]

Until now, the antibacterial mechanism of Ag-based species has not been well elucidated yet. However, there are three widely accepted mechanisms accounting for the antibacterial activity of Ag-based species to date, as follows. (1) Ag ions eluted from Ag-based species were thought to interact with phosphorus moieties in DNA,[35-38] and/or to react with thiol and amino groups of proteins,[38-40] resulting in a disruption on DNA replication, inhibition of enzyme functions and ATP production. (2) Silver ions or silver nanoparticles were considered as catalyst to catalyze dissolved oxygen for producing excess reactive oxygen species (ROS),[41] which can attack membrane lipid and resultantly give rise to an impairment on membrane integrality, mitochondrial function and DNA replication. (3) Silver ions or particles were proposed to interact with bacterial membrane and give a direct destruction of the cell membrane.[38,42]

To tentative explore mechanism of AgBr' antibacterial properties, we firstly examined the influence of AgBr nanocube on the respiratory chain enzyme of dehydrogenase by TTC-test according to chen's method.[35] (As dehydrogenase is an important enzyme in respiration chain, the disruptions on respiratory chain of *E. coli* by AgBr could be reflected by the changes on dehydrogenase activities.) To put it simply, triphenyltetrazolium chloride (TTC) is a small and colorless matter that can be ingested by live bacteria and convert to red triphenylformazane (TF) when TTC catches the hydrogen atom producing by dehydrogenase of living *E. coli*. By detecting the optical absorption of TF at 492 nm, average dehydrogenase activity of total *E. coli* could be statistically obtained. As shown in Fig.4a, the *E. coli* cells after exposure to AgBr nanocubes show much lower optical absorption value at 492 nm as compared with the control test without contact with AgBr nanocubes, illustrating an obvious decrement on dehydrogenase activity as a result of impairment of respiratory chain enzyme of dehydrogenase and/or depletion number of live bacterial cells induced by a killing effect on *E. coli*. The similar phenomenon happened on the *E. coli* cells after

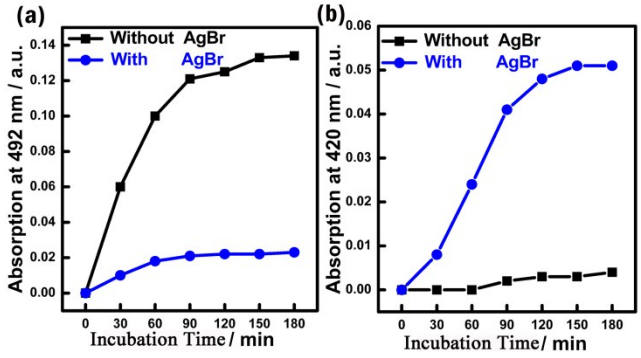

Figure 4 (a) Optical absorption changes at 492 nm on time in TTC-test. (b) Optical absorption changes at 420 nm on time in galactosidase activity test.

exposed to Ag nanoparticles has been found as well.[5,35,43] In this case, released Ag ions were considered to be able to destroy the respiratory chain dehydrogenase and resultantly deactivated the respiration to disturb normal growth and metabolism of bacteria cells, such as uncoupling of respiration from ATP synthesis.

Considering that *E. coli* cells contacted with AgBr nanocube may further suffer severe morphological changes and even cell wall destruction, leading to a leakage of intracellular contents, the influence of AgBr nanocube on integrality of *E. coli* cell wall was investigated by galactosidase activity test. Leaking of β-D-galactosidase from *E. coli* cells as a result of cell wall damage inducing by AgBr would catalyze the hydrolysis of o-nitrophenol,β-D-galactopyranoside to form o-nitrophenol, which has a characteristic absorption peak at 420 nm.[35] When β-D-galactosidase was released together with other intracellular content, absorption at 420 nm should be enhanced as formation of o-nitrophenol. Upon this, spectroscopic method could be employed to evaluate the degree of cell membrane damage induced sterilization indirectly. As shown in Fig. 4b, optical absorption at 420 nm of the control group without exposure to AgBr nanocube is near to zero and constant with incubation time, demonstrating negligible leakage of β-D-galactosidase and no changes on *E. coli* cell membrane. In a sharp contrast, co-incubation of *E. coli* cells with AgBr nanocube leads to a surge on absorption at 420 nm. This result strongly manifests that AgBr nanocube can destroy the *E. coli* cells membrane and result in an outflow of intracellular content. To give a directly evidence on this point, *E. coli* cells before and after exposure to of AgBr nanocubes were further examined by SEM observations. The normal *E. coli* cells show well cell morphology and the cell membranes are intact, as shown in Fig.5a. Compared with untreated *E. coli* cells, *E. coli* cells treated AgBr nanocubes underwent several clear structural failures, (1) size of treated *E. coli* cells is smaller than untreated ones; (2) formation of "huge holes" on the surface of membrane (marked by yellow arrows) and (3) larger portion of intercellular content looks like to be "eaten away"(Fig.5b). Destruction of cell wall membrane and shrinkage of cell volume presented above well supported the result of galactosidase activity test in terms of great damage on the cell membrane by AgBr nanocubes.[44]

Although the antibacterial mechanism of AgBr nanocube of this work has not been fully investigated, on the basis of obtained

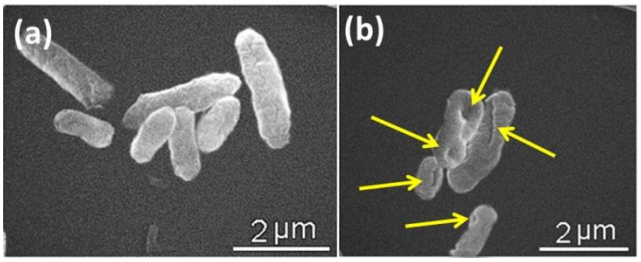

Figure 5 SEM images of (a) normal *E. coli* and (b) *E.coli* after exposure to of AgBr nanocubes.

results and previous theory, it is reasonable to propose an antibacterial mechanism to explain the enhanced antibacterial properties as follow. AgBr nanocube as a kind of sparingly soluble silver salts and facilitated by nanosized dimension tends to dissolve and generate sufficient silver ions due to the high solubility product of AgBr and high specific surface area of nanocubes. Because ionic silver is well-known for its antibacterial effect, hence, it is easily to understand that the eluted silver ions from AgBr nanocubes account for killing *E. coli* cells at least a part of antibacterial activity owing to a high affinity with DNA, proteins, enzyme, and so forth, thus affecting their correct bio-functions, such as respiratory chain reactions (proved in this work), DNA replication, and ATP production. In addition, AgBr nanocubes can also make a destructive contact with *E. coli* cell wall, and lead to a lethal destruction on membrane and outflow of intracellular bioactive components, which have been supported by galactosidase activity test of this work as well as other reported investigation. Therefore, the "dual-punch" of Ag^+ induced disturbances on bio-functions and AgBr nanocubes induced damage on cellular structure make the AgBr nanocubes to be excellent antibacterial candidate with lower MIC and MBC value.

3.2 Investigation on antibacterial activity of Ag@AgBr nanocubes

For investigating the antibacterial properties of Ag@AgBr, the obtained AgBr nanocubes were reduced by $NaBH_4$ in aqueous condition to produce metallic Ag component on the surface of AgBr and to form Ag@AgBr core-shell structure. It can be seen that the reduced sample does not inherit the cubic morphology of AgBr

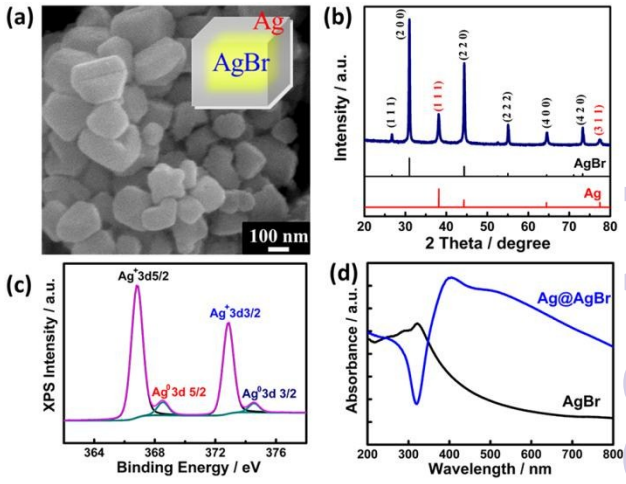

Figure 6 (a) SEM image, (b) XRD pattern, and (c) XPS spectra of Ag@AgBr. (d) UV-Vis absorption spectra of Ag@AgBr and AgBr naocube.

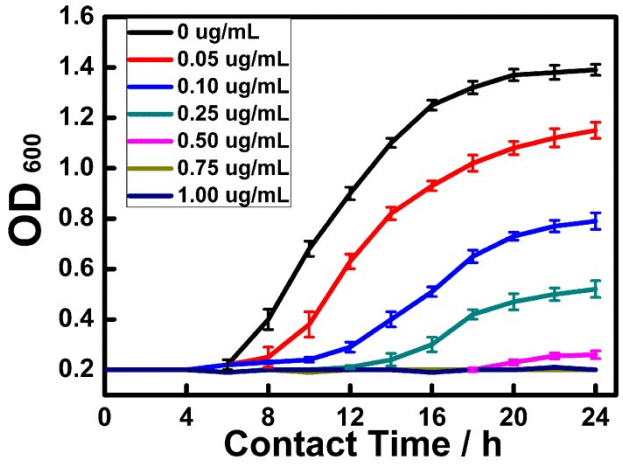

Figure 7 Growth curves of *E. coli* cells exposed to different concentrations of Ag@AgBr nanocubes (The *E. coli* bacterial grew in the nutrient broth).

precursor well, but contains some polyhedrons with a wide size distribution in the range of 60-300 nm (Fig.6a). For further investigating the nanostructure of these Ag@AgBr nanoparticles, the energy dispersive spectroscopy (EDS) analysis was performed . It can be seen from Fig.S1 that the surface composition of Ag@AgBr nanoparticles is mainly Ag element and the atomic ratio of Ag/Br is near to 5.2. As the signal of Br element may also originate from the underlay of sample, we trust the sample of Ag@AgBr is of core-shell structure with Ag on the external surface and AgBr inside, suggesting that the reduction reaction caused by $NaBH_4$ just takes place on the surface area of AgBr. The XRD characterization on the crystal phase reveals that the reduced sample do have the silver crystal phase as expected.(Fig.6b) Besides the diffractive peaks attributing to AgBr phase, the peaks at 38.09^o and 77.43^o could be definitely indexed to metallic Ag crystallographic plane of (1 1 1) and (3 1 1). Another evidence on the formation of Ag@AgBr is XPS spectra of Ag 3d core-level, in which the curve could be fitted into two spin-orbit doublets, corresponding to two different oxidation states of Ag atoms. The main peaks, having a $Ag3d_{5/2}$ at 366.8 eV and a $Ag3d_{3/2}$ at 372.8 eV, could be attributed to the Ag atoms being in a +1 oxidation state. The second doublet, with a higher binding energy but lower intensity at 368.5 eV and 374.5 eV, could be ascribed to the emission of $Ag3d_{5/2}$ and $Ag3d_{3/2}$ core levels from the Ag atoms in an oxidation state of 0 (Fig.6c). At last, the optical changes after reduction on AgBr were checked as well. As shown in Fig. 6d, Ag@AgBr composite exhibited pronounced absorption in the visible-light region as compared with that of pristine AgBr nanocubes, which is due to the localized surface plasmon resonance (LSPR) of the formed Ag nanoparticles. Taken XRD, XPS and UV-vis results together, we can firmly conclude the formation of Ag@AgBr nanostructure by reducing AgBr nanocube.

With these results in hand, we next examined the effects of metallic Ag introduction on the antibacterial activities against *E. coli* bacteria. The growth kinetics curves of *E. coli* cells exposed to different concentrations of Ag@AgBr exhibit similar trendline to that of AgBr nanocube, that is, more Ag@AgBr presence leads to better antibacterial activities on *E. coli* bacteria. According to

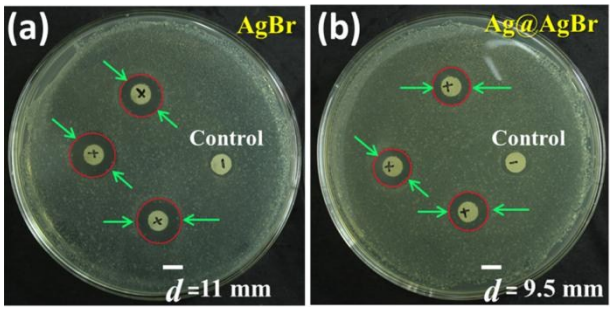

Figure 8 Optical images of the zone of inhibition for (a) AgBr and (b)Ag@AgBr.

aforementioned way in this study, the MIC and MBC values of Ag@AgBr nanoparticles against *E. coli* are determined as 0.5-0.75 μg/ml and 1 μg/ml, respectively, being higher than the MIC and MBC values of AgBr nanocube (0.1 μg/ml for MIC and 0.4 μg/ml for MBC). Although it may be due to complex factors accounting for the decline on antibacterial activities of Ag@AgBr as compared with AgBr nanocubes, we speculated that it was closely related to the reduction on the available concentration of Ag^+ to certain extent. It has been intensively reported that silver metal required the oxidation process to the Ag ion in presence of oxygen, which was a slow process and suffered low effective silver concentrations. Hence, formation of metallic Ag on the surface of AgBr will doubtlessly hinder eluting of Ag^+ from AgBr, resulting in a short of Ag ion on the whole. To support this point, we firstly studied the Ag^+ equilibrium concentration of both AgBr nanocube and Ag@AgBr nanoparticles in the nutrient broth. The equilibrium concentrations of Ag^+ for the samples of pure AgBr and Ag@AgBr tested by ICP-MS on 0.5 μg/ml suspensions after 12 h to dissolution equilibrium were 0.147 μg/l and 0.063 μg/l, respectively, implying a stronger Ag^+ releasing ability of AgBr than that of Ag@AgBr.

Afterwards, the antibacterial tests of AgBr and Ag@AgBr impregnated papers were carried out by the standard disk diffusion for further verifying the difference on Ag^+ releasing ability between them. The filters (with 5 mm in diameter) wetted by 20 μl 0.01 μg/ml AgBr or Ag@AgBr suspensions were used for this purpose. Meanwhile, the blank filters were used as control. As shown in Fig.8, the optical images of the zone of inhibition against *E. coli* show a clear zone of inhibition around each AgBr or Ag@AgBr paper disc, indicating significant antibacterial activity for both of AgBr or Ag@AgBr. The average diameters of bacteriostasis circle calculated based on three filters were 11 mm and 9.5 mm for AgBr and Ag@AgBr, further confirming the above mentioned hypothesis that AgBr is more readily to release Ag^+.

3.3 Photocatalytic antibacterial activity of AgBr and Ag@AgBr nanocubes

AgBr, as a conventional photographic material, has intensively been reported for its excellent photocatalytic performance under visible light irradiation, especially for AgBr decorated with silver nanoparticles exhibiting promoted optical properties could be used as a class of efficient plasmonic photocatalysts. Enlightened by this, the photocatalysis-assisted antibacterial activities of AgBr nanocubes and Ag@AgBr nanoparticles were tentative investigated. On the basis of previous data, we measured growth kinetics curves of *E. coli* cells with exposure to 0.2 μg/ml suspension, which is lower

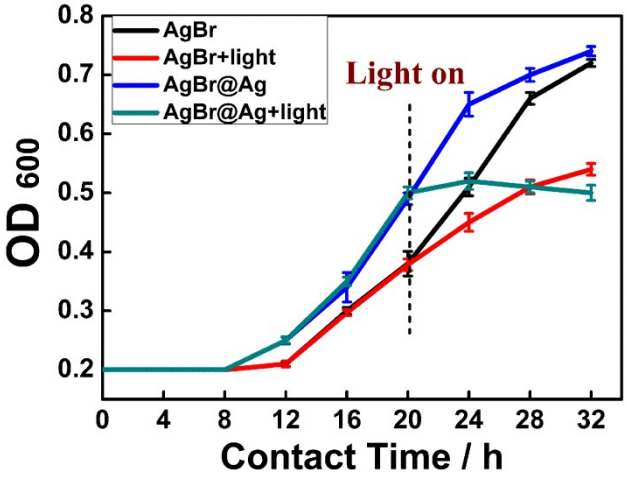

Figure 9 Growth curves of *E. coli* cells exposed to 0.2 μg/ml concentrations of AgBr or Ag@AgBr nanocubes. The visible light irradiation with wavelength of > 400 nm started at contact time of 20 h.

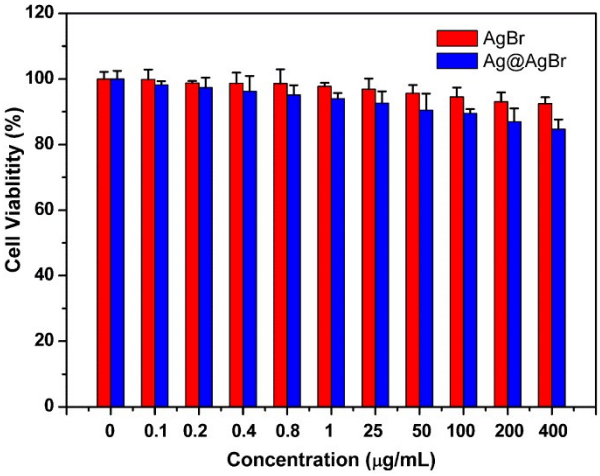

Figure 10 Cytotoxicity assay of AgBr and Ag@AgBr on L02 human hepatocytes.

than MBC value of both AgBr nanocube and Ag@AgBr nanoparticles. *E. coli* cells with exposure to 0.2 μg/ml antibacterial agent were allowed to grow in the dark for 20 h, and then the visible light was provided by a 300 W xenon lamp and wavelength was selected by a filter which only allows the light of >400 nm for the photocatalytic reaction. As shown in Fig.9, the growth curves of *E. coli* cells being exposure to either AgBr or Ag@AgBr increased remarkable with contact time within the tested 32 h if no light was provided. When the visible light irradiation was introduced at 20 h post co-incubation, the photocatalysis effect could slow down the growth rate of *E. coli* cells but could not stop it for AgBr nanocube group. In contrast, there is an obvious inhibition effect on *E. coli* cells growth under the assistance of photocatalysis in Ag@AgBr group. When it comes to photocatalytic antibacterial, it is thought that antibacterial agent absorbs light to generate electron/hole pairs, which are then captured by surface hydroxyls and oxygen molecules to produce ROS, such as superoxide anions, hydrogen peroxide, hydroxyl radicals, and singlet oxygen.[5, 30-33, 43] All of these ROS can make contributions to the antibacterial activity against *E. coli* via destruction of the cell membrane for inactivation. Benefitting from LSPR effects of Ag component, the Ag@AgBr nanostructure shows higher and wider visible light harvesting ability and is expected to produce more ROS under the irradiation. Resultantly, it accounts for higher photocatalytic antibacterial properties than its counterpart of AgBr.

3.4 Toxicity of AgBr and Ag@AgBr

Finally, the potential toxicity of AgBr and Ag@AgBr is another cased that we are concerned. As shown in Fig. 10, nearly no cytotoxicity of AgBr or Ag@AgBr nanoparticles was observed on L02 human hepatocytes at concentrations below 1.0 μg·mL^{-1}. The cell viabilities at 1.0 μg·mL^{-1} are 98% and 94% for AgBr and Ag@AgBr, respectively, indicating an excellent biological safety of AgBr as antibacterial agent that can maintain the high biocompatibility around the MIC or MBC values. This encouraging result stimulates us to perform the MTT tests at higher concentration of nanoparticles. It can be seen that even after incubation with nanocubes for 24 h at a concentration of 400 μg·mL^{-1}, cells can keep as high as 92.6 % and 84.7 % of their significant metabolic activity on AgBr and Ag@AgBr respectively. What is noteworthy, AgBr shows higher biocompatibility than Ag@AgBr. Although it is hard to make an accurate comparison between AgBr of this work and Ag-related materials as different cell types used for special research objective, we can still conclude that the AgBr nanocube of this work possesses better, at least comparable, biocompatibility than widely reported Ag nanoparticles, such as bare Ag nanoparticle of 15 nm with 20 % cell viability at 75 μg·mL^{-1},[45] PVP-coated Ag nanoparticle with 20-100% cell viability at 5-50 μg·mL^{-1},[46] citrate-coated Ag nanoparticle with 20% cell viability at 2 μg·mL^{-1}.[47] The lower toxicity of AgBr nanomaterial as compared with metallic Ag nanomaterial may be related to the less level of ROS production. Until now, numerous studies have proved the generation of ROS on metallic Ag nanomaterial and resultant oxidative stress caused Ag-induced lethal toxicity on normal human cells. This not only can well explain why AgBr nanocube has a higher Ag^+ releasing ability but shows lower cytotoxicity on normal human cells, but also can interpret that Ag@AgBr shows better photocatalytic antibacterial activities as the formation of ROS under light irradiation.

Conclusions

In summary, AgBr nanocube with a diameter around 100 nm was synthesized by precipitation reaction with PVP as capping agent at ambient temperature and then followed by a hydrothermal treatment. The antibacterial activities of AgBr on *E. coli* bacteria confirmed that the MIC and MBC values against *E. coli* were 0.1 μg/ml and 0.4 μg/ml, respectively, being better than most of previously reported Ag-based materials. The excellent disinfection property of AgBr nanocube may be due to the "dual-punch" of Ag^+ induced disturbances on bio-functions and AgBr nanocubes induced damage on cellular structure as determined by TTC-test and galactosidase activity test. Superficial modification of AgBr by metallic Ag nanoparticles led to an inhibition on eluting of Ag^+

and resultantly decreased antibacterial activities in the dark, but it favored the photocatalytic antibacterial activities owing to enhanced light harvesting ability from the LSPR effects of Ag component. Given the superior and multifunctional antibacterial activity, we expect that AgBr of this work could sever as an upcoming promising antibacterial candidate.

Acknowledgements

The financial supports from National Basic Research Program of China (2013CB932704), National Natural Science Foundation of China (Grant No. 21303033, 81373359, 91023007 and 20773033), New Century Excellent Talents in University, Outstanding Young Funding of Heilongjiang Province were gratefully acknowledged. This work is also supported by "the Fundamental research Funds for the Central Universities" (Grant No. HIT. NSRIF.2015061), Heilngjiang Postdoctoral Financial Assistance (Grant No. LBH-Z13079) and China Postdoctoral Science Foundation Funded Project (Project No.: 2014M551232).

Notes and references

‡ Footnotes relating to the main text should appear here. These might include comments relevant to but not central to the matter under discussion, limited experimental and spectral data, and crystallographic data.

1 S. Malato, P. Fernández-Ibáñez, M. I. Maldonado, J. Blanco and W. Gernjak, *Catal. Today*, 2009, **147**, 1-59.
2 J. Davies and D. Davies, *Microbiol. Mol. Biol. Rev*., 2010, **74**, 417-433.
3 R. E. W. Hancock, *Lancet Infect. Dis.*, 2005, **5**, 209-218.
4 A. J. Huh and Y. J. Kwon, *J. Control. Release*, 2011, **156**, 128-145.
5 S. Chernousova and M. Epple, *Angew. Chem. Int. Ed. Engl.*, 2013, **52**, 1636-1653.
6 J. Hasan, R. J. Crawford and E. P. Ivanova, *Trends Biotechnol.*, 2013, **31**, 295-304.
7 D. J. Newman, G. M. Cragg and K. M. Snader, *J. Nat. Prod.*, 2003, **66**, 1022-1037.
8 E. Kenawy, S. D. Worley and R. Broughton, *Biomacromolecules*, 2007, **8**, 1359-1384.
9 J. Sawai, *J. Microbiol. Methods*, 2003, **54**, 177-182.
10 M. Fang, J. H. Chen, X. L. Xu, P. H. Yang and H. F. Hildebrand, *Int. J. Antimicrob. Agents*, 2006, **27**, 513-517.
11 D. R. Monteiro, L. F. Gorup, A. S. Takamiya, A. C. Ruvollo-Filho, E. R. Camargo and D. B. Barbosa, *Int. J. Antimicrob. Agents*, 2009, **34**, 103-110.
12 M. Rai, A. Yadav and A. Gade, *Biotechnol. Adv.*, 2009, **27**, 76–83.
13 J. S. Kim, E. Kuk, K. N. Yu, and D. H. Jeong, *Nanomedicine*, 2007, **3**, 95-101.
14 B. Nowack, H. F. Krug and M. Height, *Environ. Sci. Technol.*, 2011, **45**, 1177-1183.
15 T. V. Duncan, *J. Colloid Interface Sci.*, 2011, **363**, 1-24.
16 S. W. P. Wijnhoven, W. J. G. M. Peijnenburg, C. A. Herberts, W. I. Hagens, A. G. Oomen, E. H. W. Heugens, B. Roszek, J. Bisschops, I. Gosens, D. van De Meent, S. Dekkers, W. H. De Jong, M. van Zijverden, A. J. A. M. Sips and R. E. Geertsma, *Nanotoxicology*, 2009, **3**, 109-138.
17 D. W. Brett, *Ostomy Wound Manage*, 2006, **52**, 34-41.
18 J. W. Wiechers and N. Musee, *J. Biomed. Nanotechnol.*, 2010, **6**, 408-431.
19 K. Vasilev, J. Cook and H. J. Griesser, *Expert Rev. Med. Devices*, 2009, **6**, 553-567.
20 R. Kumar, H. Münstedt, *Biomaterials*, 2005, **26**, 2081-2088.
21 R. D. Glover, J. M. Miller and J. E. Hutchison, *ACS Nano*, 201[illegible], **5**, 8950-8957.
22 M. J. Carter, K. Tingley-Kelley and R. A. Warriner, *J. Am. Acad. Dermatol.*, 2010, **63**, 668-679.
23 S. Belkhair, M. Kinninmonth, L. Fisher, B. Gasharova, C. M. Liauw, J. Verran, B. Mihailova and L. Tosheva, *RSC Adv.*, 2015 **5**, 40932-40939.
24 A. M. Pereyra, M. R. Gonzalez, T. A. Rodrigues, M. T. S. Luterbach and E. I. Basaldella, *Surf. Coat. Technol.*, 2015, **270** 284-289.
25 A. Hamad, L. Li, Z. Liu, X. L. Zhong and T. Wang, *Appl. Phys. A Mater. Sci. Process.*, 2015, **119**, 1387-1396.
26 X. H. Liu, Y. Y. Cao, H. Y. Peng, H. S. Qian, X. Z. Yang and H. B. Zhang, *CrystEngComm*, 2014, **16**, 2365-2370.
27 S. Singh, H. C. Joshi, A. Srivastava, A. Sharma and N. Verma *Colloids Surf. A Physicochem. Eng. Asp.*, 2014, **443**, 311-319.
28 X. Xiao, L. Ge, C. Han, Y. Li, Z. Zhao, Y. Xin, S. Fang, L. Wu and P. Qiu, *Appl. Catal. B*, 2015, **163**, 564-572.
29 C. An, S. Peng and Y. Sun, *Adv. Mater.*, 2010, **22**, 2570-2574
30 C. An, J. Wang, W. Jiang, M. Zhang, X. Ming, S. Wang and Q. Zhang, *Nanoscale*, 2012, **4**, 5646-5650.
31 C. An, J. Wang, C. Qin, W. Jiang, S. Wang, Y. Li and Q. Zhang, *J. Mater. Chem.*, 2012, **22**, 13153-13158.
32 J. Song, I. Lee, J. Roh, and J. Jang, *RSC Adv.*, 2014, **4**, 455[illegible] 4563.
33 H. Wang, Y. Liu, P. Hu, L. He, J. Li and L. Guo, *ChemCatChem*, 2013, **5**, 1426-1430.
34 X. Yan, X. Wang, W. Gu, , M. Wu, Y. Yan, B. Hu, G. Che, D. Han, J. Yang, W. Fan and W. Shi, *Appl. Catal. B*, 2015, **164**, 297-304.
35 S. Chen, Y. Guo, S. Chen, H. Yu, Z. Ge, X. Zhang, P. Zhang and J. Tang, *J. Mater. Chem.*, 2012, **22**, 9092-9099.
36 A. S. Kazachenko, A. V. Legler, O. V. Per'yanova and Y. A. Vstavskaya, *Pharm. Chem. J.*, 2000, **34**, 257-258.
37 J. J. Castellano, S. M. Shafii, F. Ko, G. Donate, T. E. Wright, R. J. Mannari, W. G. Payne, D. J. Smith and M. C. Robson, *Int. Wound J.*, 2007, **4**, 114-122.
38 Q. L. Feng, J. Wu, G. Q. Chen, F. Z. Cui, T. N. Kim and J. O. Kim, *J. Biomed. Mater. Res.*, 2000, **52**, 662-668.
39 H. J. Klasen, *Burns*, 2000, **26**, 117-130.
40 M. Yamanaka, K. Hara and J. Kudo, *Appl. Environ. Microbiol.*, 2005, **71**, 7589-7593.
41 Y. Matsumura, K. Yoshikata, S. Kunisaki and T. Tsuchido, *Appl. Environ. Microbiol.*, 2003, **69**, 4278-4281.
42 I. Sondi and B. Salopek-Sondi, *J. Colloid Interface Sci.*, 2004, **275**, 177-182.
43 L. Rizzello and P. P. Pompa, *Chem. Soc. Rev*., 2014, **43**, 1501-1518
44 C. Marambio-Jones and E. M. V. Hoek, *J. Nanopart. Res.*, 2010, **12**, 1531-1551.
45 C. Carlson, S. M. Hussain, A. M. Schrand, L. K. Braydich-Stolle, K. L. Hess, R. L. Jones and J. J. Schlager, *J. Phys.Chem. B*, 2008 **112**, 13608–13619.
46 Z. Wang, T. Xia and S. Liu, *Nanoscale,* 2015*,* **7***,* 7470–7481.
47 J. Shi, X. Sun, Y. Lin, X. Zou, Z. Li, Y. Liao, M. Du and H. Zhang, *Biomaterials*, 2014, **35**, 6657–6666.

